J Mater Sci (2007) 42:872–877
DOI 10.1007/s10853-006-0020-0

Microanalysis of debris formed during electrical discharge machining (EDM)

Asit Kumar Khanra · L. C. Pathak · M. M. Godkhindi

Received: 22 October 2005 / Accepted: 20 March 2006 / Published online: 11 January 2007

Abstract The present investigation attempts to focus on the influence of EDM energy input on the structure and composition of the debris that forms during machining. An indigenously prepared ZrB_2-Cu composite and mild steel plate were used as tool and workpiece (WP) material for the present study. The machining was carried out in a kerosene medium. The composition analysis of different debris particles was investigated by SEM/EDS. At low EDM energy input the SEM micrographs of WP debris showed formation of smaller size particles with few satellites. The SEM micrographs of high EDM energy input showed formation of hollow spheres, with dents, larger population of satellites, surface cracks and burnt core structures.

Introduction

The EDM is a widely used non-conventional machining process for manufacturing of dies for forging/extrusion, machining of super alloys, composites and advanced ceramics. The EDM is a thermo-electrical material removal process, in which the tool and the workpiece are connected to two electrodes and separated by a dielectric fluid. The high voltage applied induces a plasma channel between the two conductive electrodes and generates a temperature of ~20000 °C. At this condition localized evaporation of electrodes takes place in the plasma channel. The worn out material during EDM is known as debris [1–4]. The debris material is regularly swept away from the electrode surfaces by continuous flow of dielectric fluid. The debris analysis is useful to understand the material removal mechanism during the EDM and also possibly to establish a suitable process for generation of oxide free powder.

Wiley studied the debris formation at different polarities of erosion and concluded that the erosion could be due material removal through either solid or liquid or vapour forms and the formation of nonspherical particles was due to non thermal erosion mechanism [5]. Walter et al. produced several amorphous powders such as of $Fe_{97}Al_3$, $Fe_{75}Si_{15}B_{10}$, Fe_3B, Fe_2B, FeB, Fe_3Si, $Fe_{82-x}M_xB_{18}$ (M- Ni, Co, Cr, V, Pt, Mo, Si etc.) by spark erosion (EDM) technique [6–10]. They also compared the crystallization kinetics between the powder produced by spark erosion and ribbon produced by melt spinning. They claimed that spark erosion technique could produce 100% amorphous powder, which was not possible by melt spinning or atomization techniques. Walter has produced various powders of particle size 5 nm to 75 μm by spark erosion method. The power consumption of spark erosion is very less but the production rate is always slower than other powder production processes [10]. Ayers et al. have produced TiC, ZrC, WC, W_2C powders by EDM [11, 12]. The EDM was done under reverse polarity and during EDM the carbon (breakdown of dielectric) reacted with tool (Ti/Zr/W) to form

A. K. Khanra (✉) · M. M. Godkhindi
Deptartment of Metallurgical and Materials Engineering,
IIT, Kharagpur 721302, India
e-mail: asit_iitkgp@yahoo.com

L. C. Pathak
MST Division, National Metallurgical Laboratory,
Jamshedpur 831007, India

metal carbide powder. But the production rate is again very low [12]. Murthi et al. have analyzed the debris in ultrasonic assisted EDM [5]. The ultrasonic vibration leads to generation of larger particles, more collusion of particles as compared to the product with out ultrasonic vibration. The higher input current and pulse results in a higher input energy and produces larger crater dimensions, which are responsible for the larger size of debris. The effect of rotating electrode on formation of debris during EDM of titanium alloy and die steel was studied by Soni et al. [13]. The electrode rotation results in formation of finer particles. All the above studies have been carried out with copper or graphite as the tool materials, though these are attempted to replace these tools by composite materials.

In the present investigation the effect of EDM energy input on morphology and the chemical composition of debris during machining of mild steel by ZrB_2-Cu composite tool has been investigated.

Experimental procedure

In the present investigation, a well-polished mild steel (C- 0.18%) plate was used for machining by EDM (Electra, EMS 5535-R50ZNC, India). The tool was indigenously prepared by compaction and sintering. The ZrB_2 powder (99.5% pure, Alfa Aesar, Germany) was mixed with 40 wt% Cu powder (99.9% pure, Metal powder Company, India) in a polyethylene bottle for 5 h and then compressed into 6.6 mm diameter and 5 mm thickness pellets by applying uniaxial pressure of 250 MPa. The pressureless sintering of the pellet was carried out in a high temperature graphite furnace (Thermal Technology Inc.USA) at 1250 °C under a continuous flow of high purity argon gas (XL grade). After sintering a further homogenization was carried out at 1000 °C for 2 h in a tubular furnace under high purity argon gas. These sintered pellets were fixed on one end of a Cu (99.9% pure) rod by adding a conductive Ag paste and baked for 10 h at 75 °C. This composite fixed with Cu rod was used as tool material. The tool should good machining behaviour with larger MRR (metal removal rate) and lower TRR (tool removal rate) than conventional Cu tool.

The tool and WP were kept as positive and negative electrodes respectively. Fresh kerosene oil (fire point ~65 °C) was used as the dielectric fluid. The EDM was performed under three conditions: (i) low energy input (pulse on-time 5 μs), (ii) medium energy input (pulse on-time 50 μs) and high-energy input (pulse on-time 100 μs). The entire study was done at 3 amp current and 45 V gap voltage. Before EDM the dielectric chamber was cleaned properly. A small steel container (150×150 mm^2) was placed appropriately in the dielectric chamber and the WP was kept inside the small steel container. The fine dispersed debris particles with dielectric was siphoned off from this container and filtered. The filtration was repeated three times to collect the fine particles. Finally the particles were cleaned by acetone and dried. These cleaned and dried particles were analyzed by scanning electron microscope (SEM) [JEOL, JSM 840A, Japan]. The composition analysis was carried out by SEM/EDS analysis. The cleaned and dried particles were heated at 700 °C for hydrogen lost test. The MRR were calculated at the three conditions (low, medium and high energy input). The phase analysis of mild steel (WP) and tool after EDM was carried out by X-Ray Diffractometer (XRD) [PW 1840, Philips, Netherlands].

Results and discussion

The SEM images of debris particles produced under different conditions are shown in Fig. 1. The micrographs show mainly spherical particles with some non-spherical particles in all cases. The formation of spherical shape indicates the spheriodization time to be short compared to solidification time. The average particle size slightly increases from pulse on-time of 5–50 μs and then significant increase is found at pulse on-time of 100 μs.

A careful analysis of the structure of the debris indicates it to consist mainly of a large number of spherical particles with a dispersion of few non-spherical particles. An examination at higher magnification further indicates the non-spherical particle to consist of a large number of smaller irregular particles in a continuous matrix while spherical particles seem to be single phase structure with signs of dendritic internal growth. The EDS analyses of the spherical and non-spherical particles also show significant differences (Fig. 2). The spherical particles are rich in Fe with significant amount of Cu and some Zr (Table 1) where as the non-spherical particles are very rich in Zr and Cu and contain minor quantities of Fe. The EDS analysis is not sensitive to B, C or O (light elements). One can, however, reasonably conclude that the spherical particles could originate from WP where as the non-spherical particles are generated through the erosion of tool materials. There is also evidence of

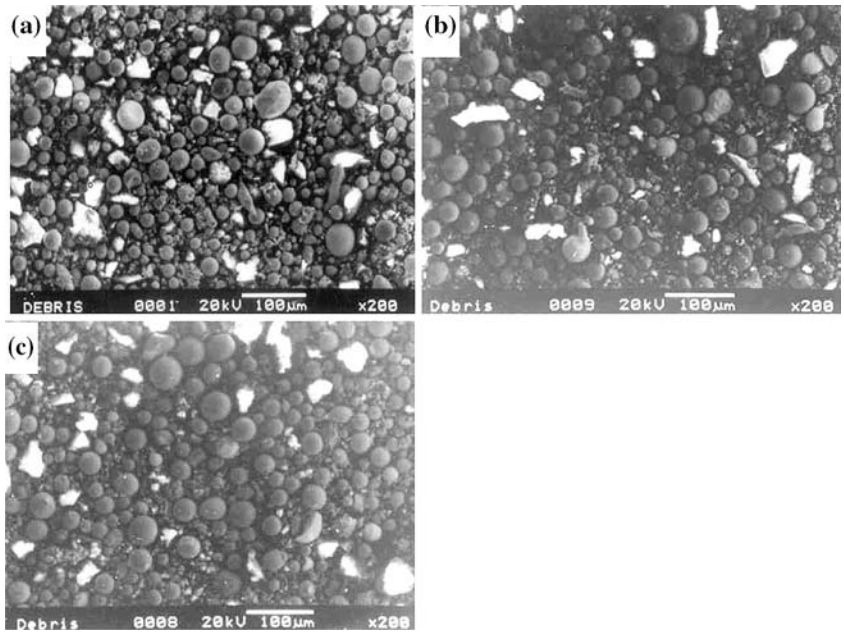

Fig. 1 SEM images of debris at different conditions: **a–c**-pulse on-time 5, 50, and 100 µs respectively

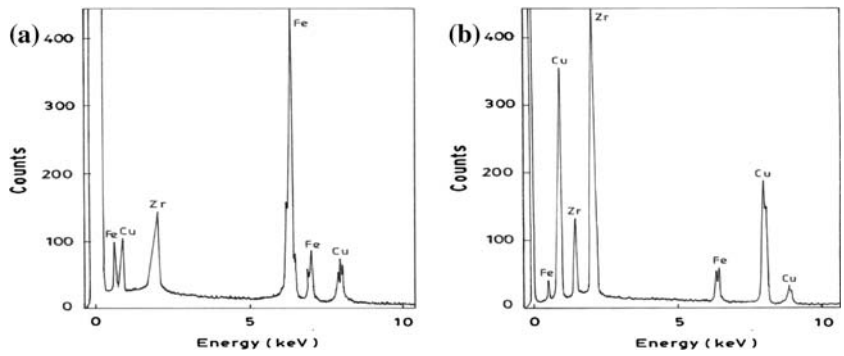

Fig. 2 EDS analysis: (**a**) spherical particle; and (**b**) non-spherical particle

Table 1 Bulk EDS analysis of debris at different conditions

EDM condition	Element (wt %)		
	Fe	Cu	Zr
Pulse on-time–5 µs	53.73	33.89	12.38
Pulse on-time–50 µs	54.36	34.22	11.42
Pulse on-time–100 µs	56.20	35.71	8.09

Table 2 Weight loss by H_2 reduction at different conditions

EDM condition	Weight Loss (%)
Pulse on-time–5 µs	0.11
Pulse on-time–50 µs	0.15
Pulse on-time–100 µs	0.19

significant transfer of WP material (Fe) to tool and tool material (ZrB_2-Cu composite) to WP.

The MRR at three different conditions are found to be ~0.01, 0.05 and 2.52 mg/min for pulse on-time of 5, 50, 100 µs respectively. The TRR is very negligible and the MRR reflects the production rate of debris. The table 2 shows the weight loss during reduction at 700 °C by H_2. This observed weight loss is due to reduction of iron and copper oxide, which are present in the debris. The weight loss increases with the pulse on-time, which indicates the rate reaction of Fe or Cu with the oxygen. This source of oxygen could be dissolved air in the dielectric media or occluded air during agitation. The XRD pattern of WP (at pulse on-time of 100 µs) shows presence of residual austenite (γ) as a minor phase with the major ferrite (α) (Fig. 3). This indicates the ferrite transformation into austenite and reverse transformation during cooling. The presence of austenite is found in all three cases. So the presence of austenite phase in the debris is expected. Similarly the XRD pattern of tool surface shows formation of ZrC phase after EDM, which indicates presence of ZrC phase in the debris (Fig. 4). During

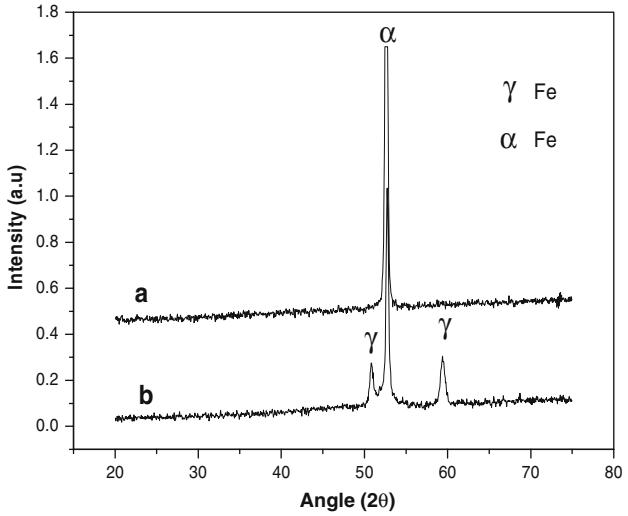

Fig. 3 The XRD patterns of workpiece: (**a**) before EDM and (**b**) after EDM

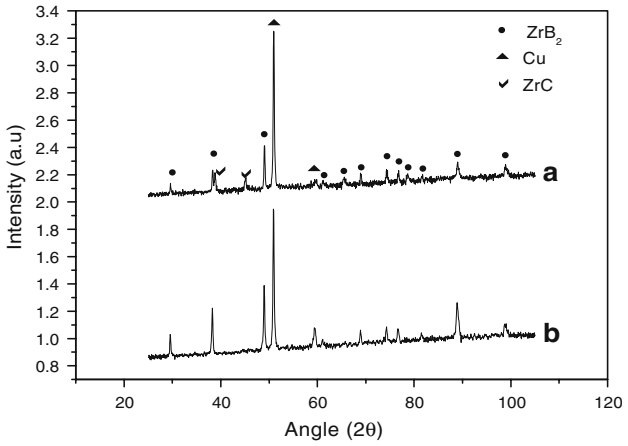

Fig. 4 The XRD patterns of tools: (**a**) after EDM and (**b**) before EDM

EDM due to high temperature the ZrB_2 could partially dissociate into Zr and B and then the Zr and C react to form ZrC. But no boron carbide formation is observed during the EDM. The amount of ZrC phase in debris may be low as the TRR is much lower than MRR.

The difference in the morphology of debris from WP and tool are indicative of the difference in the mechanism of their formation. The spherical particles (WP debris) would form through the solidification of the vapour phase emanating from WP where as the debris from tool material gets generated through the layer by layer thermal spalling. The tendency for spalling increases with increased input energy. The generation of high temperature during EDM also cause evaporation and decomposition of kerosene causing significant carbon deposition on the WP as well as tool material [14].

The morphology of various debris collected during low energy input EDM is shown in Fig. 3. The non-spherical particles (Fig. 5D) are clearly produced through the thermal spalling of the tool material and appear to be composite mixture of ZrB_2 particles embedded in a metal (predominantly Cu) matrix. The spherical particles can be concluded to have been produced through the vapour phase condensation mainly from the WP (see chemical analysis in Table 1 and Fig. 2A). The spheres appear solid and have an occasional condensation of a satellite particle (Fig. 5B, C). Many of the spherical surfaces also show typical dendritic structures indicating a sufficiently slow rate of cooling.

Microstructural features of the medium and high-energy input EDM (Figs. 6 and 7) are similar, but there is a higher population of satellite, the spheres appear to be dented (Fig. 7D, E). While the spheres show typical dendritic structure with lower dendritic size (Fig. 6B, C), they also appear to be hollow with surface cracks (Fig. 6C). The spherical particles produced at higher energy input levels often appear as burst open with a blackened core; a typical burnt structure. The satellite population as well as the severity of dents seems to increase with increasing energy input.

One can attempt to understand the various features in terms of material removal mechanism during EDM. During the process of EDM due to the generation of the spark very high temperatures (~20000 °C) are generated locally for a very short time period. The intensity of spark would increase with increased energy input. The localized generation of high temperatures would cause localized melting and evaporation of the metallic phase and thermal decomposition of the boride phase and also evaporation and decomposition of the dielectric medium (kerosene). Since the dielectric medium is kept in continuous circulation, the electrodes will be cooled, but the vapour streams will become turbulent. Due to the turbulence the vapour stream will disintegrate into smaller fractions and each fraction will tend to condense into liquid (liquid metal and liquid kerosene) and subsequently into solid particles. The presence of a vapour blanket of kerosene tends to reduce the cooling rate of the liquid metal droplets, which help in spheroidisation as well as dendritic segregation. When the energy input is low the vapour content is low and thus we get fewer particles and of smaller average size. They also solidify faster and thus appear to be more solid. When the energy input increases the vapour stream will break into

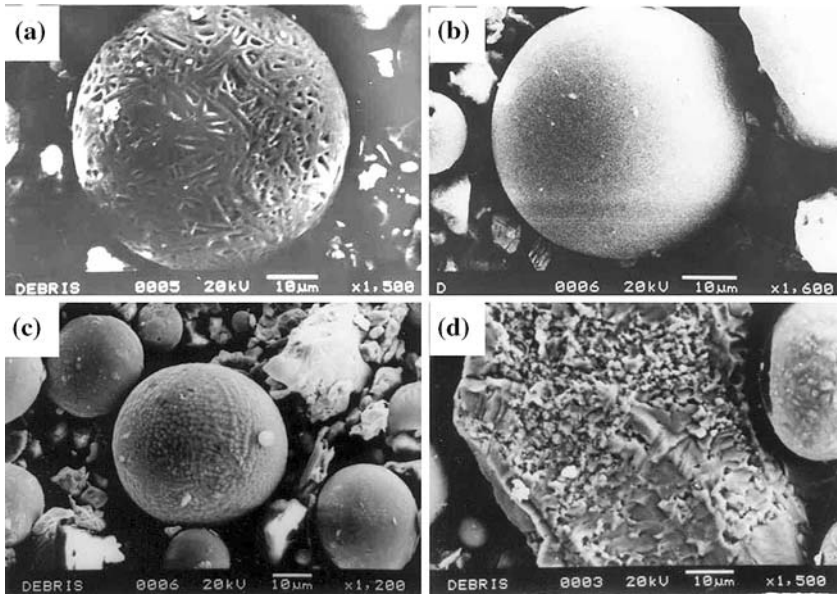

Fig. 5 SEM images of debris at low energy input (pulse on-time 5 µs): (**a**) typical dendritic structure; (**b**) solid sphere; (**c**) satellite formation; and (**d**) non spherical particle

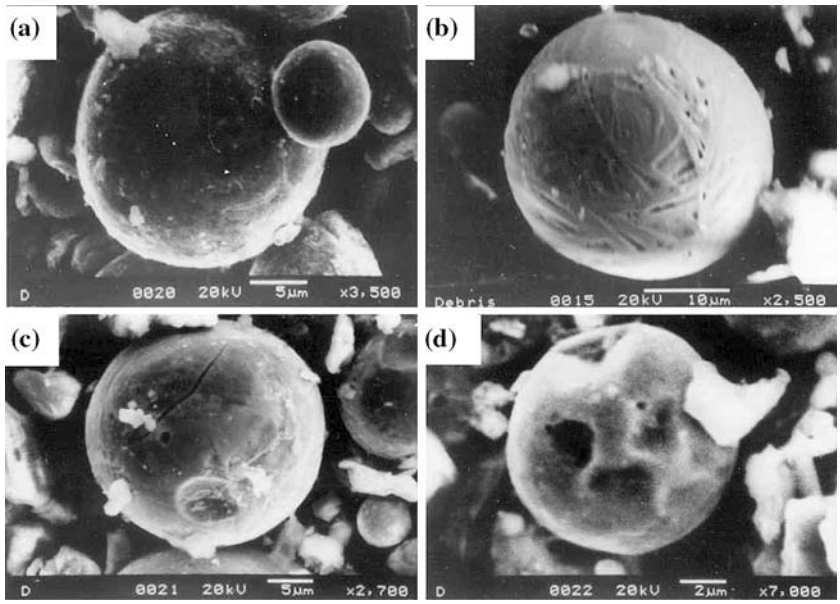

Fig. 6 SEM images at medium energy input (pulse on-time 50 µs): (**a**) satellite; (**b**) dendritic structure; (**c**) dent with crack; (**d**) typical dent formation)

larger volumes tend to occlude much of dielectric vapour (kerosene vapour and gaseous decomposition products of kerosene) cool slower, tend to collide with each other (due to turbulent flow of kerosene medium) and in the process develop dents and cracks. When collision occurs between a larger semi solid sphere and a smaller solidified sphere typical satellite structure is formed. Due to the occuled gases they tend to become hollow. When the energy input is high, the entrapped kerosene vapor would tend to decompose and deposite a layer of carbon giving rise to the typical burnt structure.

Conclusions

(1) The EDM debris consists of two types of particles. A combined analysis of shape and EDS indicates spherical particle to consist of mainly WP material and nonspherical particles are generated from tool material. The average particle size seems to increase with energy input.

(2) The debris from WP is generated through high temperature evaporation of WP and subsequent solidification whereas the debris from tool is generated through thermal spalling.

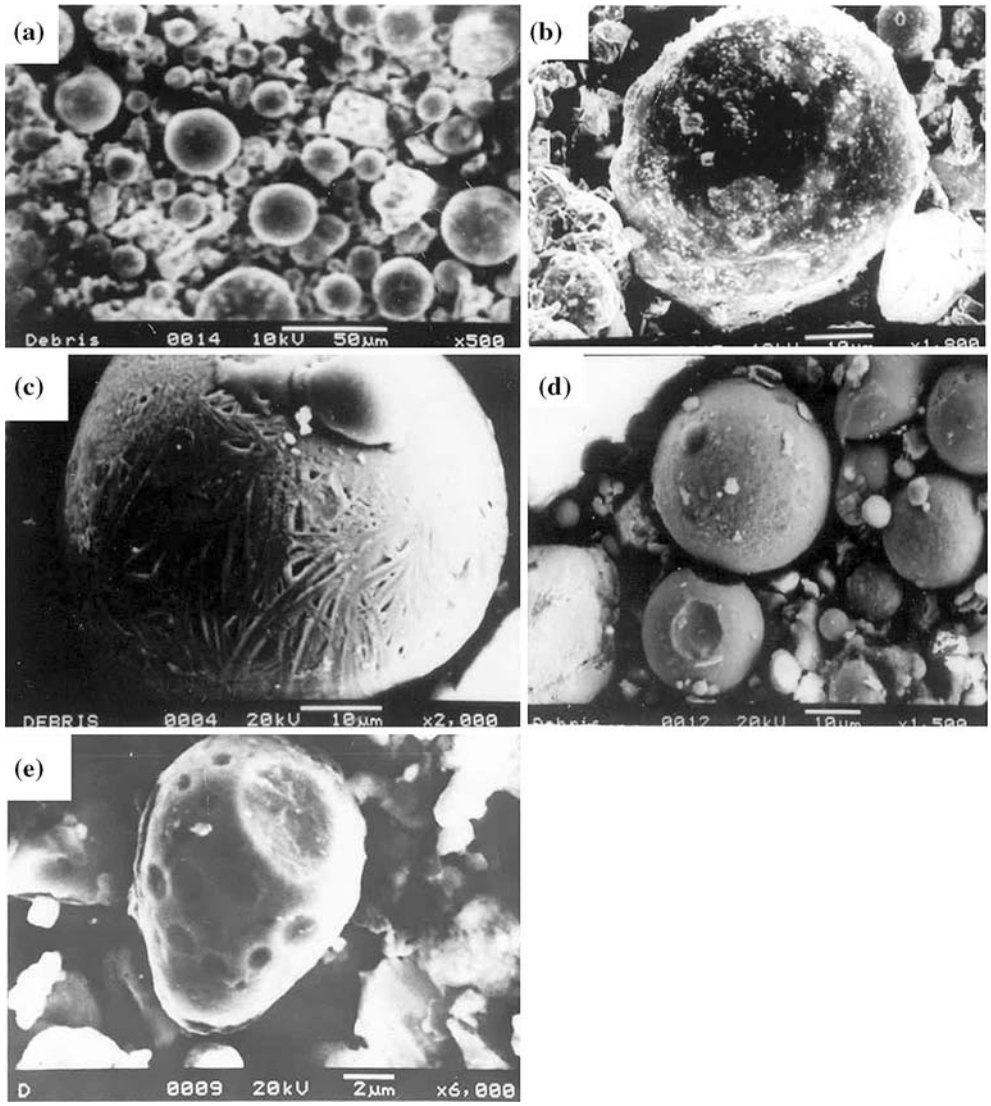

Fig. 7 SEM images at high energy input (pulse on-time 100 µs): (**a**) Debris and **b**, **c**, **d**, **e** are selected image of particle of debris (**b** hollow sphere, **c** dendritic structure, **d** satellite with dent formation, **e** typical dent formation)

(3) Attempts are made to explain the morphological features of the debris (satellite, dents, cracks and burnt core) in terms of the basic processes during the solidification of vapours generated due to sparking.
(4) The XRD analysis of the WP after EDM indicates that the WP surface temperature could rise sufficiently to cause $\alpha \rightarrow \gamma$ transformation and similarly the tool surface may get sufficiently heated for formation of ZrC to take place.

Acknowledgements Authors are thankful to Mr. S. Sahana of IIT Kharagpur, India for help in carrying out SEM. Authors are also grateful to Prof. A. K. Chakraborty and Prof. A. B. Chattopadhyay of IIT Kharagpur, India for valuable discussion regarding debris analysis.

References

1. Ho KH, Newman ST (2003) Int J Mach Tools Manuf 43:1287
2. Singh S, Maheshwari S, Pandey PC (2004) J Mater Process Technol 149:272
3. Petrofes NF, Gadalla AM (1988) Ceram Bull 67:1048
4. Norasetthekul S, Eubank PT, Bradley WL, Bozkurt B, Stucker S (1999) J Mat Sci 34:1261
5. Murthi VSR, Philip PK (1987) Wear 117:241
6. Walter JL, Berkowitz AE, Koch EF (1983) Mat Sci Engg 60:31
7. Walter JL (1981) Mat Sci Engg 50:137
8. Walter JL, Berkowitz AE (1984) Mat Sci Engg 67:169
9. Berkowitz AE, Walter JL (1982) Mat Sci Engg 55:275
10. Walter JL (1988) Powder Met 31:267
11. Ayers JD (1983) Metall Trans A 14A:5
12. Ayers JD, Moore K (1984) Metall Trans A 15A:1117
13. Soni JS (1994) Wear 177:71
14. Cabanillas ED, Desimoni J, Punte G, Mercader RC (2000) Mat Sci Engg A 142A:163